



## Simulation Coordination Control of PV And Battery On Microgrid With PI Controller

Adhi Kusmanto<sup>1\*</sup>, Takashi Hiyama<sup>2</sup>

<sup>1</sup>Electrical Engineering Department, Faculty of Engineering and Informatics, Universitas PGRI Semarang, Indonesia

<sup>2</sup>Department of Computer Science and Electrical Engineering, Faculty of Engineering, Kumamoto University, Japan

### Abstract.

**Purpose:** The output power of PV (photovoltaic) changes according to changes in the intensity of solar radiation. Therefore, the purpose of this study is to use a utility grid connected system to overcome changes in solar energy sources and loads. This is done to maintain an uninterrupted power supply to the load.

**Methods:** In this study, we propose a grid-connected PV system with several DC-DC converters connected in parallel with several PV sources and batteries with PI control coordination. The proposed method includes two stages, namely the DC-DC converter development stage and the battery management strategy stage.

**Result:** The study results show that within 0 seconds to 0.45 seconds the DC bus is supplied with PV. Due to the change in PV, within 0.45 seconds to 0.65 seconds the DC bus is supplied with unit-1 battery. When there is a change in the unit-1 battery, within 0.65 seconds to 0.8 seconds the DC bus is supplied with the unit-2 battery. By using PV coordination arrangements and battery units, the microgrid can still supply power to the load even if changes occur in the PV or grid.

**Novelty:** The novelty in this study is a new microgrid configuration to increase the demand for electrical loads. The new configuration uses multi-PV and multi-battery. Multi-PV is used to supply the load and is stored in the multi-battery, while multi-battery is used at night and if there is a disturbance at the PV output.

**Keywords:** PI controller, Coordinated control, Microgrid, DC bus

**Received** April 2023 / **Revised** April 2023 / **Accepted** May 2023

*This work is licensed under a [Creative Commons Attribution 4.0 International License](https://creativecommons.org/licenses/by/4.0/).*



### INTRODUCTION

Indonesia is a tropical area that has the potential to use solar panels (PV) to meet electricity needs. The On-Grid system is the most widely used grid-connected PV system and the system works when the utility source is available. This system model is a simple system and can help during peak loads during the day. In this case the system works effectively when the intensity of solar radiation is at its peak. A grid-connected PV system can send excess PV-generated power to utilities. Initially this system was designed not to use batteries, but along with technological developments and the need for electric power, this system was designed in a hybrid manner with off-grid systems or using batteries [1].

In the control coordination strategy system [2], [3] to overcome AC bus power fluctuations a fuzzy logic control is used on two battery units. Other studies related to grid connected PV systems [4],[5] carried out coordinating the reactive power output of wind turbines with other reactive sources for increased voltage stability. In the proposed strategy, the voltage levels on the DC-link are segmented to differentiate converter operation. When the DC-link voltage is within safe limits, the PV source operates in MPPT mode and the inverter output frequency is programmed in proportion to the DC-link voltage deviation. Y.Du et al. (2020). [6] presents microgrids with different distributed generators (DG) connected to the distribution network. A system energy management (EMS) algorithm was implemented to coordinate the operations of different DG units for grid and island connected operations. To improve power management, [7] coordination of inverters and two-way DC-DC converters is carried out based on the State of Charge (SoC) of the battery so that MPPT and power injection are achieved simultaneously. To increase Active Power balancing in grid-connected PV, [8],[9] is carried out with barycentric coordination on a cascaded fed H-bridge converter. When the voltage drop approaches 80% of the nominal voltage, the converter is able to supply

---

\* Corresponding author.

Email addresses: [adhikusmanto@upgris.ac.id](mailto:adhikusmanto@upgris.ac.id) (Kusmanto)

DOI: [10.15294/sji.v10i2.43929](https://doi.org/10.15294/sji.v10i2.43929)

an active power flow of 810 W. Research on the coordination of PV reactive power control connected to the grid [10], with a supply of 6 KVAR shows the line resistivity exceeds a certain critical value, so that compensation becomes less effective. But by taking into account the active and reactive power the system becomes more effective [11].

Other related research, namely researcher [12] used decentralized control coordination for DC bus voltage regulation and power sharing from several PV sources. This method is also used [13] in coordinated control of PV and EV located at different locations in a radial network connected to the microgrid. However, this method has not been able to cope with changes in load. Other researchers [14] proposed a distributed control structure to manage energy in a microgrid system autonomously, while [15],[16] used a distribution control with a battery which plays an important role in the voltage regulation process, to overcome PV power fluctuations. For the purpose of improving the performance of T-NPC type inverters in grid connected PV systems, a passive based decoupling control scheme was proposed [17]. With 10 kW prototype demonstrating the proposed control scheme is effective. Researcher [18] proposed a multilayer control coordination method in AC energy management of grid-connected microgrids. This strategy predicts customer load demand and PV a day ahead. Meanwhile, researchers [19] use multiple energy stores to be able to meet demand at load. Research [20] presents a coordination scheme of DC microgrid ring voltage regulation coordination with energy hubs (EH), namely battery banks, fuel cells. This method utilizes the converter and EH in a coordinated manner, to maintain the voltage at the load terminals within tolerance limits. In the end the research conducted [21],[22] used the voltage regulation method for distribution network systems, the method used taking into account the optimization of utility reactive power and reducing the problem of ramp-rate use of high voltage PV. The distributed voltage control method was tested on an unbalanced medium voltage feeder, with active and reactive power regulation of the inverter.

Based on previous research, for a grid-connected PV system, multi DC-DC converters are used which are connected in parallel with several PV sources. Control coordination using PI controller. A part from being connected to the grid via a solar inverter, the PV output is also connected to the battery. The goal is that at night the PV does not output power, so the battery is connected to the grid via a battery inverter. With this method the system can help overcome peak loads during the day and night.

The following methods are widely used for grid connected PV systems. When there is a sudden change in radiation intensity, the PV output power ( $P_{pv}$ ) will decrease. In order to maintain the DC voltage at the desired value, the inverter must reduce the amount of load. The power reduction from the inverter supplied to the grid can be avoided by adjusting the mismatch between the inverter power and the power generated by the PV. Therefore during sudden changes in solar radiation, the battery unit converter control signal must be set so that the battery pack provides power to overcome the difference. This can be expressed by equation (1) as follows

$$P_{inv} = P_b + P_{pv} \quad (1)$$

If the grid voltage is low, the PV must remain connected to the grid for a minimum period of time and must provide reactive power [23]. In this case the inverter is controlled using a vector control strategy where the q axis precedes  $\pi/2$  with respect to the d axis. The active and reactive power of the inverter are expressed in equations (2) and (3) as follows

$$P_{inv} = \frac{3}{2} [v_{gd} i_d + v_{gq} i_q] \quad (2)$$

$$Q_{inv} = \frac{3}{2} [v_{gq} i_d + v_{gd} i_q] \quad (3)$$

where ( $v_{gd}$ ,  $v_{gq}$ ) and ( $i_d$ ,  $i_q$ ) are the grid voltage and grid current, respectively, to the grid side inductor of the LCL filter in a rotating reference frame (RRF). Usually, the d axis of the RRF is oriented along the grid voltage using the PLL, so  $v_{gd} = V_g$ ,  $v_{gq} = 0$ . Therefore the active and reactive power delivered by the inverter is expressed equation (4) as follows:

$$P_{inv} = \frac{3}{2} v_g i_d \quad (4)$$

$$Q_{inv} = -\frac{3}{2} v_g i_q \quad (5)$$

In equation (5) shows that the component q controls the reactive current and at low voltage. References to the reactive component of the current are denoted by  $i_q^*$ . Since the active power of the inverter equation (5) does not come from the DC-link voltage controller, it is necessary to maintain a balance of power on the DC-link to avoid over-voltage. Low voltage inverter reference values are currents  $i_d^*$  dan  $i_q^*$ , so the control architecture used is current control or PI controller. Figure 1 shows the PV control connected to the utility grid.

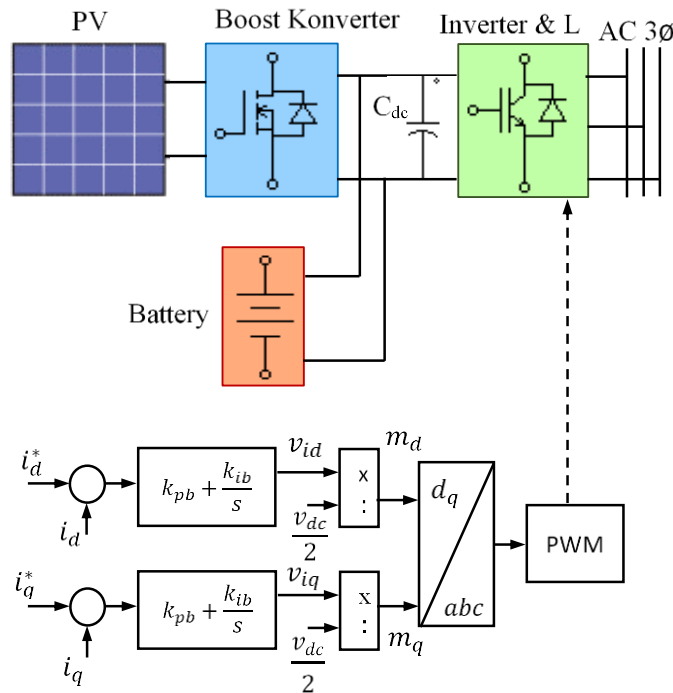


Figure 1. Grid connected PV control

The PI parameter setting of the plant transfer function ( $G(s)$ ) is determined by the filter. The PI control is considered as an inductive filter ( $L_f$ ), consisting of two filters ( $L_1$  and  $L_2$ ). This is because the plant gain in controlling bandwidth does not change significantly for LCL and equivalent filter  $L$ . The feedforward compensation, d-axis and q-axis in  $G(s)$  can be expressed by equation (6) as follows

$$G(s) = \frac{1}{sL_f + R_f} \quad (6)$$

$R_f$  is the parasitic resistance of the filter  $L$ . Since the system is a first-order system, the control gain can be selected based on the position of the pole-zero. Furthermore, because the plant transfer function is the same, proportional gain and integral gain can be expressed by equation (7) as follows

$$k_p = \frac{L_f}{\tau_i} \quad (7)$$

Where  $\tau_i$  is the required bandwidth, with a current magnitude of 0.5 ms-5 ms [24]. The bidirectional DC-DC converter is used to connect the battery to the PV, shown in Figure 2. The inductor ( $L$ ) filter on the bidirectional DC-DC converter is designed [25] based on the maximum allowable current ripple ( $\delta_i$ ). Minimum inductance value during charge and discharge mode with equation (8) as follows

$$L = \frac{1}{6f_k} \frac{V_{dc}^2}{\delta_i P_O} \quad (8)$$

where  $f_k$  is the switching frequency and  $V_{DC}$  is the DC-link voltage.

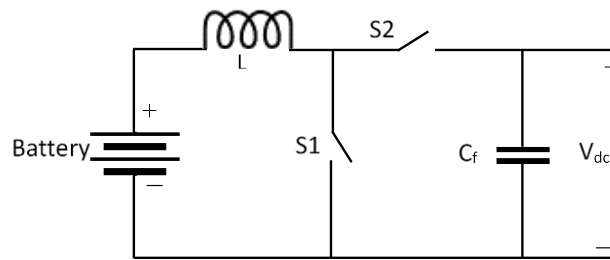


Figure 2. DC-DC bidirectional converter

**METHODS**

The proposed PV and battery coordination system with PI controller in a microgrid includes two stages, namely the DC-DC converter development stage and the regulatory strategy stage on the battery side. The system proposed in the block diagram is shown in Figure 3. The system consists of two PV units and two battery units. The system is connected to the 220 V utility grid.

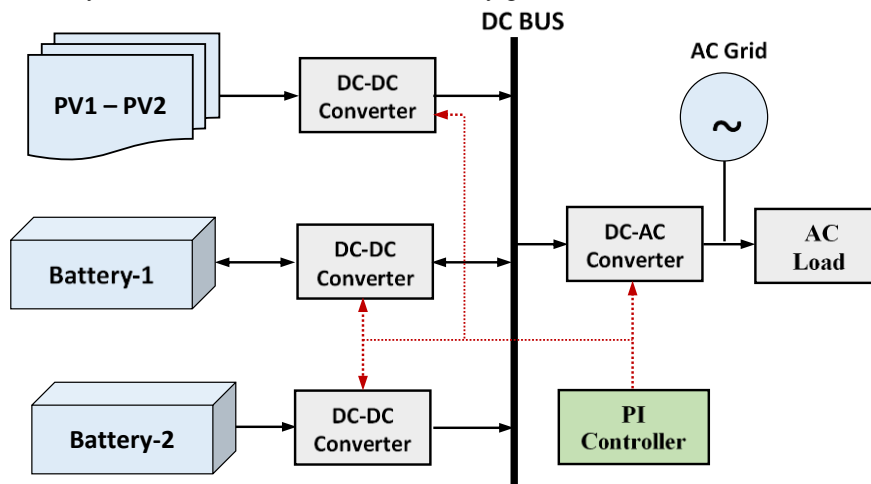


Figure 3. PI controller coordination block diagram

**A. Multi DC-DC Converter Design**

In this first phase, the development of DC-DC converters with outputs for inverters and batteries is carried out. In this stage, the PV output is also stored in the battery apart from being used as inverter input. In this stage, three converters are used, each connected to the input inverter, battery-1 and battery-2, as shown in Figure 4. Meanwhile, PV1 consists of 5 PV modules connected in parallel. Likewise, for the number of PV2 modules. In the design, PV1 and PV2 are connected in series, so the direct output voltage from PV1 and PV2 is 24 V. In the figure, the PV output is not only used as an inverter input. It is also stored in battery-1 and battery-2. The parameters of for each PV module are shown in Table 1.

Table 1. Solarex MSX-60 PV module parameters

Specifications	Value
Number of Cells $N_s$	36
Standard Light Intensity $S_0$	1000 W/m <sup>2</sup>
Ref. Temperature $T_{ref}$	25 °C
Series Resistance $R_s$	0.008 Ω
Shunt Resistance $R_{sh}$	1000 Ω
Short Circuit Current $I_{sc0}$	3.8 A
Saturation Current $I_{s0}$	2.16 e <sup>-8</sup> A
Band Energy $E_g$	1.12 eV
Ideality Factor $A$	1.2
Temperature Coefficient $C_t$	0.0024 A/°C

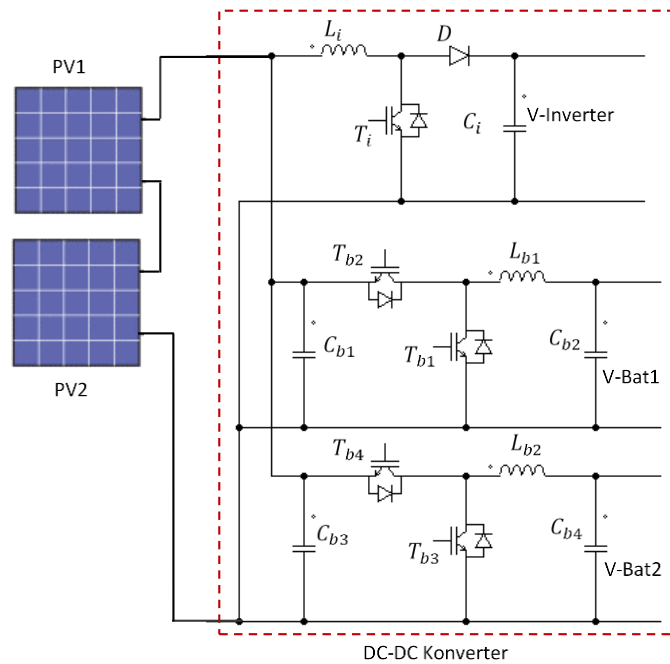


Figure 4. DC-DC converter design

The storage system uses two battery units. Each battery unit uses ten batteries connected in parallel, so that the output voltage in the same direction is 12 V. The battery uses a bidirectional converter. When the charging process occurs, the PV output DC voltage is lowered from 24 V to 12 V. When the battery discharging process or PV does not provide DC output power, the battery converter will increase the DC voltage from 12 V to 24 V. Table 2 shows the battery parameters used in this research.

Table 2. Li-ion battery parameters

Specifications	Value
No. of Cells in Parallel/ Seri	1
Rated Voltage	12 V
Discharge Cut-off Voltage	1000 $\Omega$
Rated Capacity	100 Ah
Internal Resistance	0.05 $\Omega$
Discharge Current	1.08 A

### B. Battery Control Design

In this stage, the strategy for setting the battery unit-1 and battery-2 units is carried out in supplying energy to the DC bus. The control scheme for the one and two battery units is shown in Figure 5. PI controller is used for each bidirectional converter.

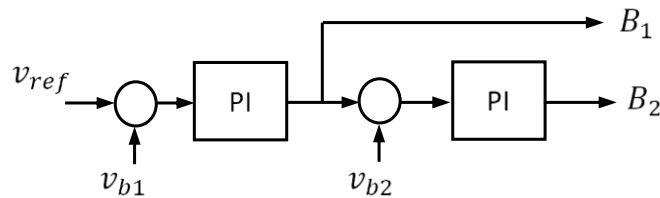


Figure 5. Battery control design

The  $V_{ref}$  voltage is the reference DC voltage at battery-1 and battery-2 as the input source of the converter. When the PV source is disconnected, battery 1 supplies the DC bus. When battery-1 is disconnected or the stored energy is reduced, battery-2 supplies the DC bus. The inverter (DC/AC converter) converts DC voltage to AC voltage to supply to the grid or AC load. Figure 6 shows the PV unit and battery coordination algorithm in distributing power to the DC bus. Figure 6 shows the coordination algorithm for PV and battery control in a microgrid system.

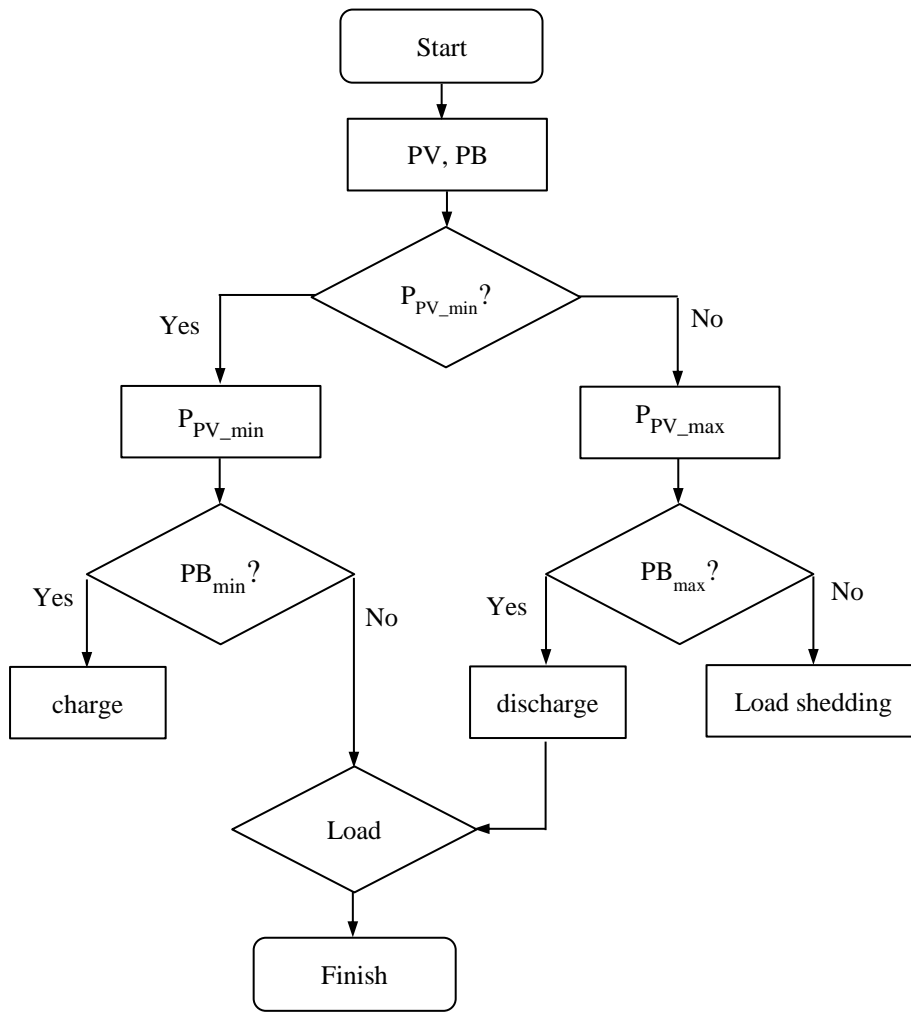


Figure 6. Microgrid control coordination

## RESULT AND DISCUSSION

At the beginning of this study, a DC bus arrangement was carried out with a PV source and two battery units. At the beginning of the PV source, apart from being connected to the grid via an inverter, some of the energy was also stored in two battery units. The PV used consists of 5 PV modules. The module used is Solarex MSX-120, the capacity of each PV module is 120 Wp with an open circuit voltage ( $V_{oc}$ ) 21.1 V. Figure 7 shows the intensity of solar radiation of  $1000 \text{ W/m}^2$ , while Figure 8 shows the characteristics of the PV module with radiation of  $750 \text{ W/m}^2$  at  $25^\circ\text{C}$ .

Radiation Intensity

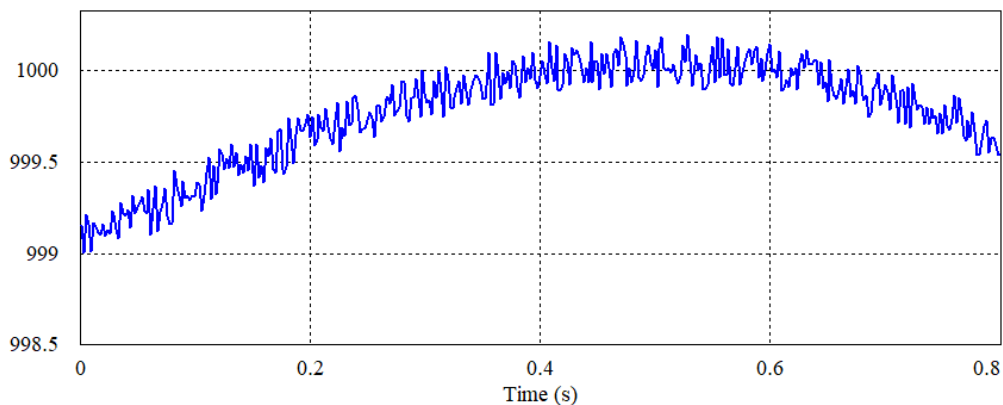


Figure 7. Solar radiation  $1000 \text{ W/m}^2$ ,  $25^\circ\text{C}$

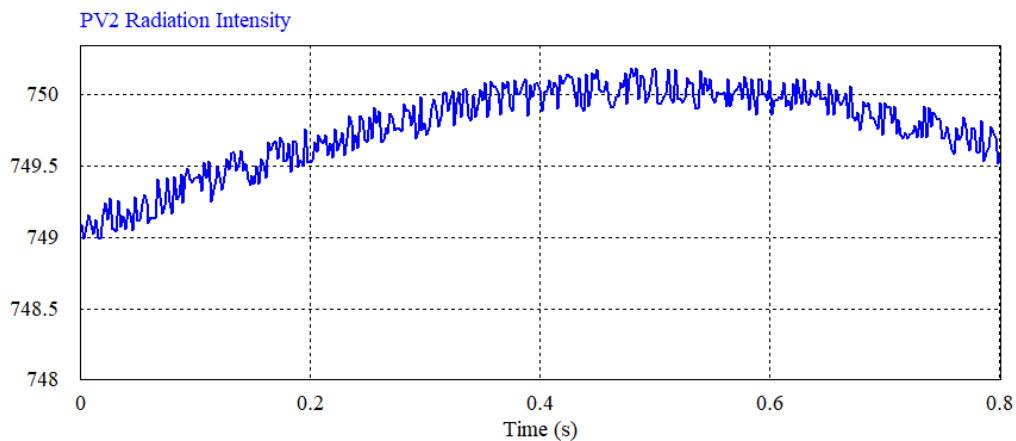


Figure 8. Solar radiation 750 W/m<sup>2</sup>, 25 °C

By using the solarex MSX-120 PV module, a test was previously carried out in the form of PV characteristics. These characteristics are the power-voltage characteristics and the current-voltage characteristics with a radiation intensity of 1000 W/m<sup>2</sup>, which can be seen in Figure 9 and Figure 10.

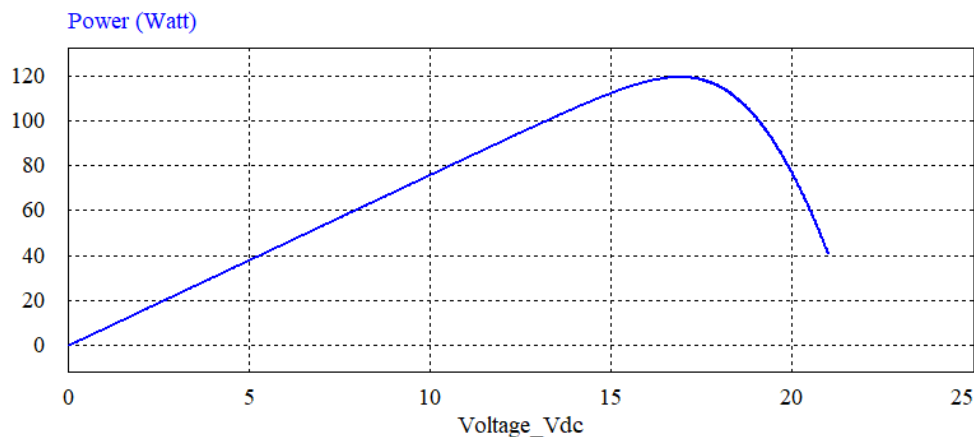


Figure 9. P-V characteristics

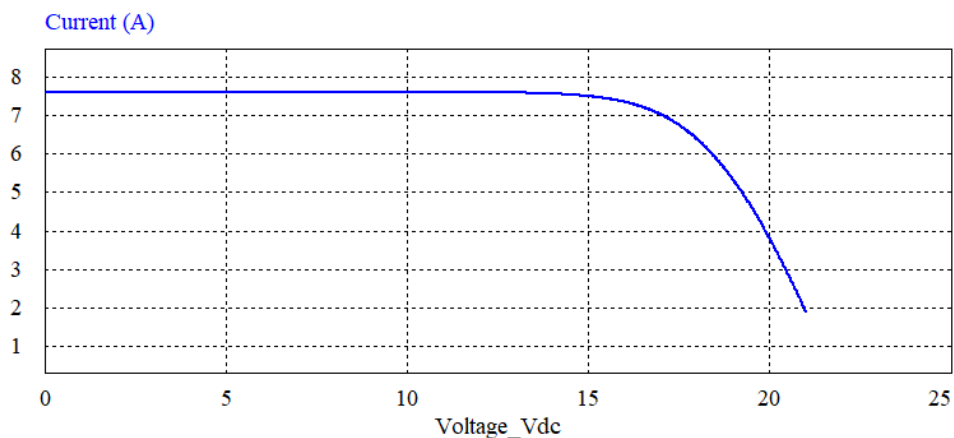


Figure 10. I-V characteristics

The PV output voltage of 24 V is reduced by 12 V for charging the battery unit using a bidirectional converter. When the battery is needed to supply the DC bus, each battery unit coordinately provides 12 V as input to the converter. This converter will increase the voltage according to the DC bus voltage, which is 24 V. The purpose of this model is to stabilize the voltage on the DC bus, so that it can supply power to the load and excess power to the grid. The method used provides DC voltage to the DC bus as shown in

Figure 11. Voltage 1 is the battery voltage, while voltage 2 is the voltage that has been increased by the converter by 24 V (DC bus voltage). Meanwhile, Figure 12 shows that voltage 1 is the PV output voltage, while voltage 2 is the PV converter voltage (24 V).

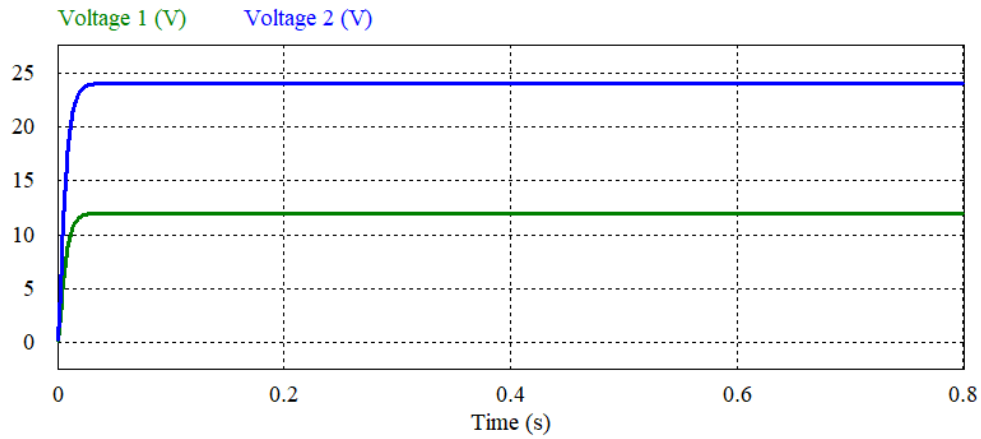


Figure 11. Battery voltage and DC bus

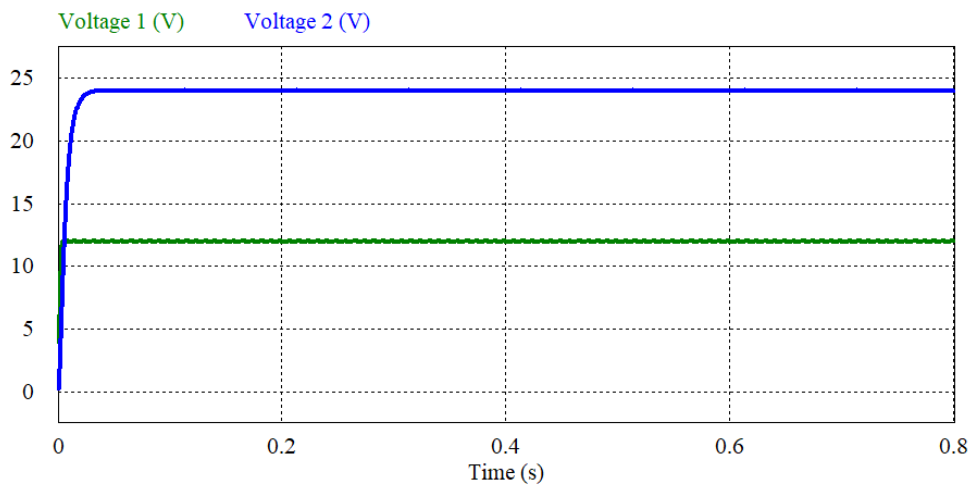


Figure 12. PV and DC bus voltages

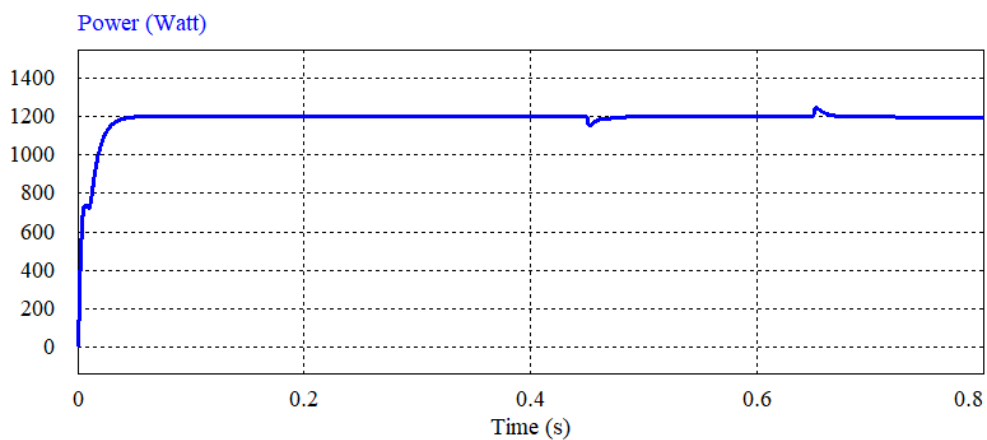


Figure 13. Coordination control of PV and battery output power

Figure 13 shows the change in power supplied from the PV and the battery pack. Within 0 seconds to 0.45 seconds the power on the DC bus is supplied by the PV source. As a result of a change in the PV source, within 0.45 seconds to 0.65 seconds the DC bus is supplied with battery unit 1. When a change occurs in battery unit-1 due to a decrease in power, then within 0.65 seconds to 0.8 seconds the DC bus is supplied with battery unit 2. Based on the design results model to overcome the problem of changing the source in the DC bus can be done by using the coordination of PV and battery units. Sources from DC bus and AC grid, separately supply power to AC loads. By changing the PV source, the microgrid system design is able to provide a DC bus voltage of 24 V.

Figure 14 shows the power output of PV1 and PV2 as node A, each PV1 and PV2 delivering 600 watts of power. Meanwhile, the output power of the battery converter-1 is node B and the output power of the battery converter-2 is node C. The output power of node B is 1200 watts, so is node C.

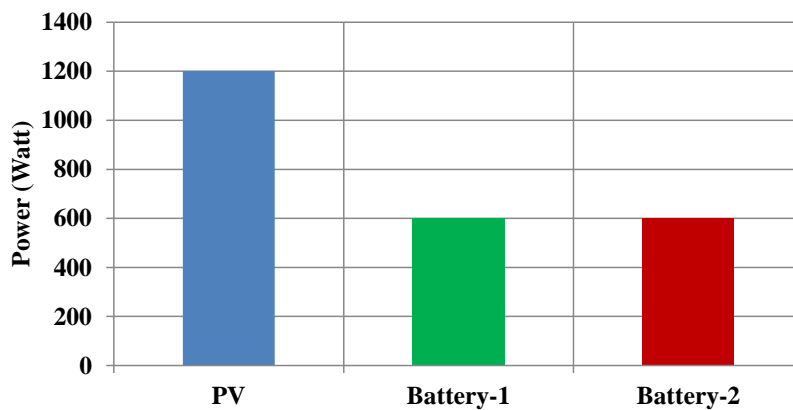


Figure14. Microgrid resource capacity

The load used is the load used in residential homes. The loads used are supplied from single-phase grids and microgrid sources via inverters. In a grid-connected PV system, the inverter's output AC voltage is in phase with the AC grid voltage. The grid voltage is with an amplitude of 220 V, while the inverter output voltage is with an amplitude of 218 V AC. This can be seen in Figure 15. In addition, Figure 16 shows the output current with the source from the inverter output. This current is the load current, which is 4.7 A.

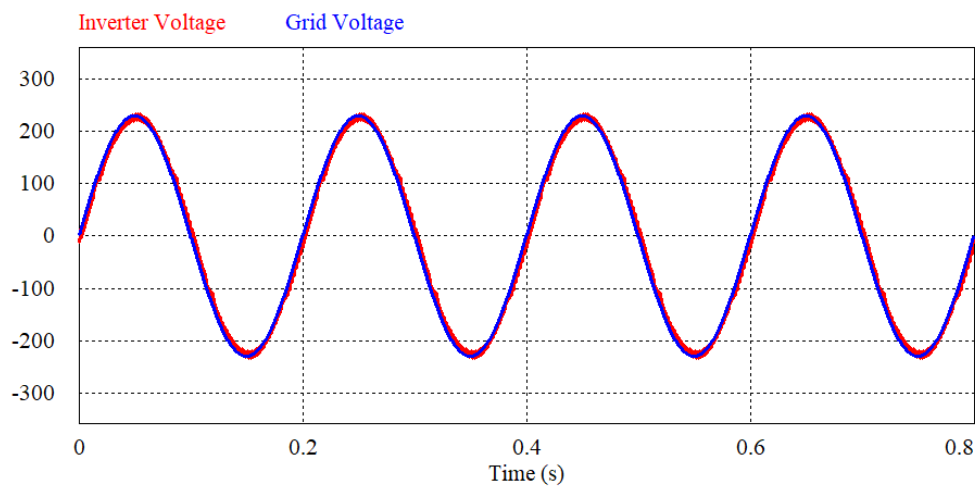


Figure 15. Grid and inverter AC voltage

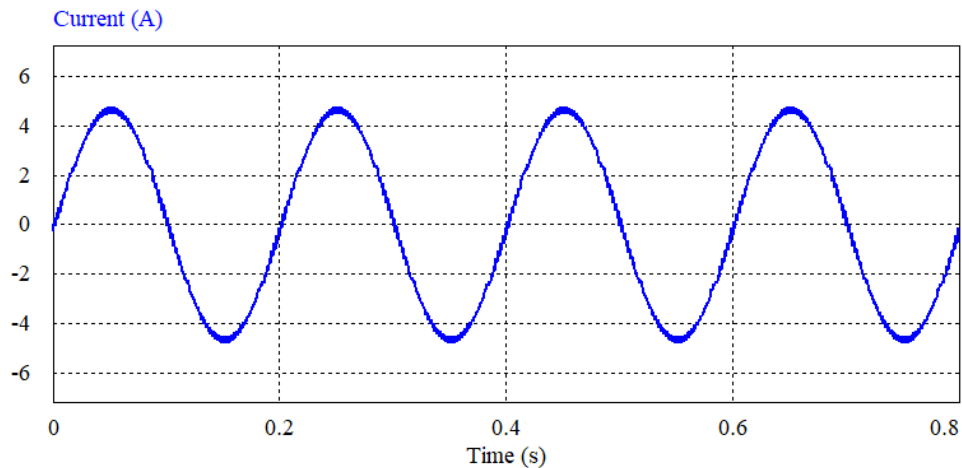


Figure 16. Load output current

Table 3. Comparison of power flow to load

Load	Load Energy	Microgrid Energy	Grid Energy
	Wh	Wh	Wh
6W LED light	72	54	18
10W LED lamp	90	75	15
12 W fan	108	95	13
Computer	105	94	11
Water pump	110	99	11
Electric stove	100	93	7

Table 3 above shows a comparison of the power consumption from the microgrid with the power from the utility grid. From the table it can be seen that PV sources and batteries can meet the load power flow, while the power flow from the utility grid is very low. This shows that control coordination with PI controller is able to lighten the electricity load on the utility grid. The results of the study found a new microgrid configuration to increase the demand for electricity loads. The new configuration uses multi-PV and multi-battery. Multi-PV is used to supply the load and is stored in multi-batteries, while multi-battery is used at night and if there is an interruption at the PV output.

## CONCLUSION

The output power of PV (photovoltaic) changes according to changes in the intensity of solar radiation. To overcome fluctuations in PV power, a control strategy is implemented to maintain power supply to the microgrid. Therefore, a utility grid connected system is used to cope with load changes and renewable energy sources on the microgrid, so that an uninterrupted power supply is generated to the load. The power or DC bus voltage can be set with a hybrid system between PV and battery units. Meanwhile, load regulation is carried out using a hybrid system between grids and inverter output. The PI controller coordination system model between the PV and battery units can provide power to the DC bus. Based on testing, within 0 seconds to 0.45 seconds, the DC bus power is supplied using a PV source. When there is a change in the PV source from 0.45 seconds to 0.65 seconds, the DC bus is supplied by battery unit 1. When there is a decrease in power on the battery unit-1, then within 0.65 seconds to 0.8 seconds, the DC bus is supplied by battery unit 2. This method can be developed by microgrid multiple source control strategy with a grid from PLTD.

## REFERENCES

- [1] S. Xu, R. Shao, B. Cao, and L. Chang, "Single-phase grid-connected PV system with golden section search-based MPPT algorithm," *Chinese J. Electr. Eng.*, vol. 7, no. 4, pp. 25–36, 2021, doi: 10.23919/CJEE.2021.000035.
- [2] A. Buchori, A. Kusmanto, A. Burhanuddin, and T. Hiyama, "Hybrid Water Feedback Solutions Using Internet of Thing ( Iot ) Enabled Water Pumps Powered by Solar Panels," *Sci. J. Informatics*, vol. 10, no. 1, pp. 55–68, 2023, doi: 10.15294/sji.v10i1.41007.
- [3] A. Kusmanto, A. Priyadi, V. L. Budiharto Putri, and M. Hery Purnomo, "Coordinated Control of Battery Energy Storage System Based on Fuzzy Logic for Microgrid with Modified AC Coupling

- Configuration,” *Int. J. Intell. Eng. Syst.*, vol. 14, no. 2, pp. 495–510, 2021, doi: 10.22266/ijies2021.0430.45.
- [4] M. Mao, “Decentralized Coordination Power Control for Islanding Microgrid Based on PV/BES-VSG,” *CPSS Trans. Power Electron. Appl.*, vol. 3, no. 1, pp. 14–24, 2018, doi: 10.24295/cpsstpea.2018.00002.
- [5] D. Yang, X. Wang, F. Liu, K. Xin, Y. Liu, and F. Blaabjerg, “Adaptive reactive power control of PV power plants for improved power transfer capability under ultra-weak grid conditions,” *IEEE Trans. Smart Grid*, vol. 10, no. 2, pp. 1269–1279, 2019, doi: 10.1109/TSG.2017.2762332.
- [6] Y. Du, X. Lu, H. Tu, J. Wang, and S. Lukic, “Dynamic Microgrids with Self-Organized Grid-Forming Inverters in Unbalanced Distribution Feeders,” *IEEE J. Emerg. Sel. Top. Power Electron.*, vol. 8, no. 2, pp. 1097–1107, 2020, doi: 10.1109/JESTPE.2019.2936741.
- [7] N. Tong *et al.*, “Coordinated Sequential Control of Individual Generators for Large-Scale DFIG-Based Wind Farms,” *IEEE Trans. Sustain. Energy*, vol. 11, no. 3, pp. 1679–1692, 2020, doi: 10.1109/TSTE.2019.2936757.
- [8] H. Myneni and S. K. Ganjikutta, “Energy Management and Control of Single-Stage Grid-Connected Solar PV and BES System,” *IEEE Trans. Sustain. Energy*, vol. 11, no. 3, pp. 1739–1749, 2020, doi: 10.1109/TSTE.2019.2938864.
- [9] H. Khan, S. J. Chacko, B. G. Fernandes, and A. Kulkarni, “Reliable and Effective Ride-Through Controller Operation for Smart PV Systems Connected to LV Distribution Grid under Abnormal Voltages,” *IEEE J. Emerg. Sel. Top. Power Electron.*, vol. 8, no. 3, pp. 2371–2384, 2020, doi: 10.1109/JESTPE.2019.2918620.
- [10] D. Li and C. N. M. Ho, “Decentralized PV-BES Coordination Control with Improved Dynamic Performance for Islanded Plug-n-Play DC Microgrid,” *IEEE J. Emerg. Sel. Top. Power Electron.*, vol. 9, no. 4, pp. 4992–5001, 2021, doi: 10.1109/JESTPE.2020.3039266.
- [11] X. Sun, J. Qiu, and J. Zhao, “Real-Time Volt/Var Control in Active Distribution Networks with Data-Driven Partition Method,” *IEEE Trans. Power Syst.*, vol. 36, no. 3, pp. 2448–2461, 2021, doi: 10.1109/TPWRS.2020.3037294.
- [12] Y. Zhang and W. Wei, “Decentralized coordination control of PV generators, storage battery, hydrogen production unit and fuel cell in islanded DC microgrid,” *Int. J. Hydrogen Energy*, vol. 45, no. 15, pp. 8243–8256, 2020, doi: 10.1016/j.ijhydene.2020.01.058.
- [13] R. El Helou, D. Kalathil, and L. Xie, “Fully Decentralized Reinforcement Learning-Based Control of Photovoltaics in Distribution Grids for Joint Provision of Real and Reactive Power,” *IEEE Open Access J. Power Energy*, vol. 8, no. March, pp. 175–185, 2021, doi: 10.1109/OAJPE.2021.3077218.
- [14] G. Dehnavi and H. L. Ginn, “Distributed Load Sharing among Converters in an Autonomous Microgrid Including PV and Wind Power Units,” *IEEE Trans. Smart Grid*, vol. 10, no. 4, pp. 4289–4298, 2019, doi: 10.1109/TSG.2018.2856480.
- [15] K. Mahmud, M. S. Rahman, J. Ravishankar, M. J. Hossain, and J. M. Guerrero, “Real-Time Load and Ancillary Support for a Remote Island Power System Using Electric Boats,” *IEEE Trans. Ind. Informatics*, vol. 16, no. 3, pp. 1516–1528, 2020, doi: 10.1109/TII.2019.2926511.
- [16] Y. Yao, F. Ding, K. Horowitz, and A. Jain, “Coordinated Inverter Control to Increase Dynamic PV Hosting Capacity: A Real-Time Optimal Power Flow Approach,” *IEEE Syst. J.*, vol. 16, no. 2, pp. 1933–1944, 2022, doi: 10.1109/JSYST.2021.3071998.
- [17] H. Wang, Q. Huang, and Z. S. Li, “A Dynamic Bayesian Network Control Strategy for Modeling Grid-Connected Inverter Stability,” *IEEE Trans. Reliab.*, vol. 71, no. 1, pp. 75–86, 2022, doi: 10.1109/TR.2021.3063492.
- [18] Z. Ma *et al.*, “Multilayer SOH Equalization Scheme for MMC Battery Energy Storage System,” *IEEE Trans. Power Electron.*, vol. 35, no. 12, pp. 13514–13527, 2020, doi: 10.1109/TPEL.2020.2991879.
- [19] S. M. Hosseini, R. Carli, and M. Dotoli, “Robust Optimal Energy Management of a Residential Microgrid under Uncertainties on Demand and Renewable Power Generation,” *IEEE Trans. Autom. Sci. Eng.*, vol. 18, no. 2, pp. 618–637, 2021, doi: 10.1109/TASE.2020.2986269.
- [20] Y. Zhang, Q. Sun, J. Zhou, L. Li, P. Wang, and J. M. Guerrero, “Coordinated Control of Networked AC/DC Microgrids with Adaptive Virtual Inertia and Governor-Gain for Stability Enhancement,” *IEEE Trans. Energy Convers.*, vol. 36, no. 1, pp. 95–110, 2021, doi: 10.1109/TEC.2020.3011223.
- [21] E. Sanchez-Sanchez, D. Gros, E. Prieto-Araujo, F. Dorfler, and O. Gomis-Bellmunt, “Optimal Multivariable MMC Energy-Based Control for DC Voltage Regulation in HVDC Applications,” *IEEE Trans. Power Deliv.*, vol. 35, no. 2, pp. 999–1009, 2020, doi:

- 10.1109/TPWRD.2019.2933771.
- [22] X. Hu, Z. W. Liu, G. Wen, X. Yu, and C. Liu, "Voltage Control for Distribution Networks via Coordinated Regulation of Active and Reactive Power of DGs," *IEEE Trans. Smart Grid*, vol. 11, no. 5, pp. 4017–4031, 2020, doi: 10.1109/TSG.2020.2989828.
  - [23] D. Generation and E. Storage, "Amendment 1: To Provide More IEEE Standard for Interconnection," 2020.
  - [24] N. Palla and V. Seshadri Sraavan Kumar, "Coordinated Control of PV-Ultracapacitor System for Enhanced Operation under Variable Solar Irradiance and Short-Term Voltage Dips," *IEEE Access*, vol. 8, pp. 211809–211819, 2020, doi: 10.1109/ACCESS.2020.3040058.
  - [25] P. Naresh and V. S. S. Kumar, "Control of an Ultracapacitor-Based Energy Storage System for Source and Load Support Applications," *IEEE Trans. Energy Convers.*, vol. 36, no. 3, pp. 2079–2087, 2021, doi: 10.1109/TEC.2020.3045134.